Molecular Cancer Therapeutics

Ranpirnase (Frog RNase) Targeted with a Humanized, Internalizing, Anti–Trop-2 Antibody Has Potent Cytotoxicity against Diverse Epithelial Cancer Cells

Chien-Hsing Chang[1,2], Pankaj Gupta[1], Rosana Michel[1], Meiyu Loo[2], Yang Wang[1], Thomas M. Cardillo[1], and David M. Goldenberg[3]

Abstract

Ranpirnase (Rap), an amphibian RNase, has been extensively studied both preclinically and clinically as an antitumor agent. Rap can be administered repeatedly to patients without any untoward immune response, with reversible renal toxicity reported to be dose limiting. To enhance its potency and targeted tumor therapy, we describe the generation of a novel IgG-based immunotoxin, designated 2L-Rap(Q)-hRS7, comprising Rap (Q), a mutant Rap with the putative N-glycosylation site removed, and hRS7, an internalizing, humanized antibody against Trop-2, a cell surface glycoprotein overexpressed in variety of epithelial cancers. The immunotoxin was generated recombinantly by fusing Rap(Q) to each of the two hRS7 light (L) chains at the NH_2 terminus, produced in stably transfected myeloma cells, purified by Protein A, and evaluated by a panel of *in vitro* studies. The results, including size-exclusion high-performance liquid chromatography, SDS-PAGE, flow cytometry, RNase activity, internalization, cell viability, and colony formation, showed its purity, molecular integrity, comparable affinity to hRS7 for binding to several Trop-2–expressing cell lines of different cancer types, and potency to inhibit growth of these cell lines at nanomolar concentrations. In addition, 2L-Rap (Q)-hRS7 suppressed tumor growth in a prophylactic model of nude mice bearing Calu-3 human non–small cell lung cancer xenografts, with an increase in the median survival time from 55 to 96 days ($P < 0.01$). These results warrant further development of 2L-Rap(Q)-hRS7 as a potential therapeutic for various Trop-2–expressing cancers, such as cervical, breast, colon, pancreatic, ovarian, and prostate cancers. *Mol Cancer Ther; 9(8); 2276–86. ©2010 AACR.*

Introduction

RNases, in particular, ranpirnase (Rap; ref. 1) and its more basic variant, amphinase (2), are potential antitumor agents (3). The extensively studied Rap (4) has recently completed a randomized phase IIIb clinical trial, which compared the effectiveness of Rap plus doxorubicin with that of doxorubicin alone in patients with unresectable malignant mesothelioma, with the interim analysis showing that the MST for the combination was 12 months, whereas that of the monotherapy was 10 months (5). Rap can be administered repeatedly to patients without any untoward immune response, with reversible renal toxicity reported to be dose limiting (6, 7).

Authors' Affiliations: [1]Immunomedics, Inc. and [2]IBC Pharmaceuticals, Inc., Morris Plains, New Jersey; and [3]Garden State Cancer Center, Center for Molecular Medicine and Immunology, Belleville, New Jersey

Note: Supplementary material for this article is available at Molecular Cancer Therapeutics Online (http://mct.aacrjournals.org/).

Corresponding Author: David M. Goldenberg, Garden State Cancer Center, 520 Belleville Avenue, Belleville, NJ 07109. Phone: 973-844-7002; Fax: 973-543-0607. E-mail: dmg.gscancer@att.net

doi: 10.1158/1535-7163.MCT-10-0338

Conjugation or fusion of Rap to a tumor-targeting antibody or antibody fragment is a promising approach to enhance its potency, as first demonstrated for LL2-onconase (8), a chemical conjugate comprising Rap and LL2, a murine anti-CD22 monoclonal antibody (mAb), and subsequently for 2L-Rap-hLL1-γ4P (9), a fusion protein comprising Rap and hLL1, a humanized anti-CD74 mAb (10). The method for generating 2L-Rap-hLL1-γ4P allowed us to develop a series of structurally similar immunotoxins, referred to in general as 2L-Rap-X, all of which consist of two Rap molecules, each connected through a flexible linker to the NH_2 terminus of one light chain (L chain) of an antibody of interest (X). We have also generated another series of immunotoxins of the same design, called 2L-Rap(Q)-X, by substituting Rap with its nonglycosylation form, designated as Rap(Q) to denote that the potential glycosylation site at Asn^{69} is changed to Gln (or Q, single letter code). For both series, we made the IgG as either IgG1(γ1) or IgG4(γ4), and to prevent the formation of IgG4 half molecules (11), we converted the serine residue in the hinge region (S^{228}) of IgG4 to proline (γ4P). The schematic structure of 2L-Rap-X or 2L-Rap (Q)-X is shown in Fig. 1A. This design is dictated by the requirement of a pyroglutamate residue at the NH_2 terminus of Rap for the RNase to be fully functional (12).

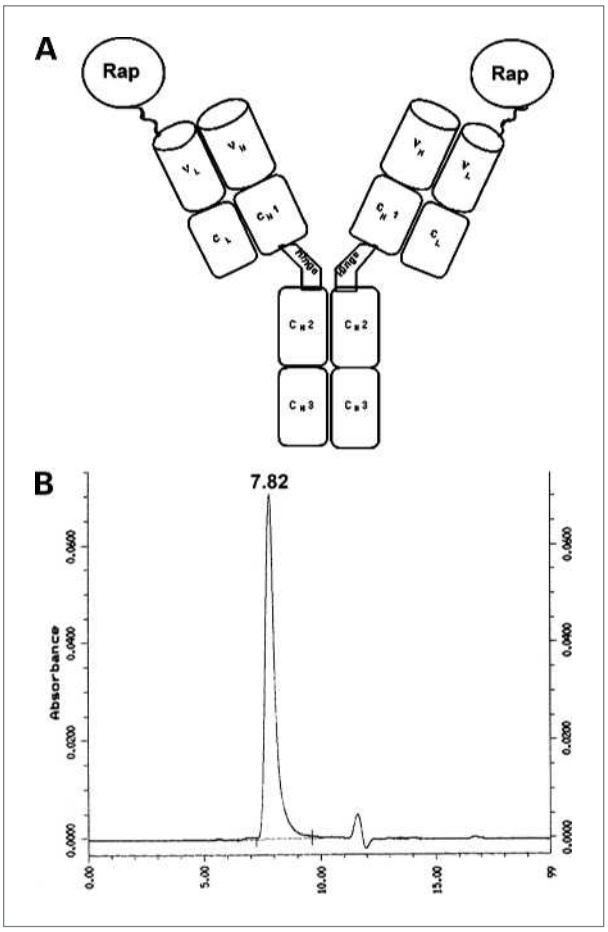

Figure 1. Molecular design and size of (Q)-hRS7. A, schematic structure of 2L-Rap-X in which X is an IgG and Rap can be Rap(Q). B, SE-high-performance liquid chromatography analysis of protein A-purified (Q)-hRS7 showing a single peak at 7.8 min.

Trop-2 is a type I transmembrane protein and has been cloned from both human (13) and mouse cells (14). In addition to its role as a tumor-associated calcium signal transducer (15), the expression of human Trop-2 was shown to be necessary for tumorigenesis and invasiveness of colon cancer cells, which could be effectively reduced with a polyclonal antibody against the extracellular domain of Trop-2 (16). The growing interest in Trop-2 as a therapeutic target for solid cancers (17) is attested by further reports that documented the clinical significance of overexpressed Trop-2 in breast (18), colorectal (19, 20), and oral squamous cell (21) carcinomas. The latest evidence that prostate basal cells expressing high levels of Trop-2 are enriched for *in vitro* and *in vivo* stem-like activity is particularly noteworthy (22).

The murine anti–Trop-2 mAb, mRS7, was generated by hybridoma technology using a crude membrane preparation derived from a surgically removed human primary squamous cell carcinoma of the lung as immunogen (23). Immunoperoxidase staining of frozen tissue sections indicated that the antigen defined by mRS7 is present in tumors of the lung, stomach, bladder, breast, ovary, uterus, and prostate, with most normal human tissues being unreactive (24). The antigen recognized by mRS7 was later shown to be a 46- to 48-kDa glycoprotein and named epithelial glycoprotein-1, or EGP-1 (25), which is also referred to in the literature as Trop-2 (15) and other names (16, 18). Upon binding to the target cells, mRS7 is rapidly internalized within 2 hours (24). Radiolabeled mRS7 has been shown to effectively target and treat cancer xenografts in nude mice in several earlier studies (26–28). To further explore the utility of mRS7 as a potential therapeutic for solid cancers expressing Trop-2, humanized RS7 (hRS7) was made by grafting the complementarity-determining regions of mRS7 onto human IgG1 frameworks (29) and fused to Rap(Q), resulting in 2L-Rap(Q)-hRS7, which is abbreviated (Q)-hRS7 hereafter.

We have previously reported that 2L-Rap-hLL-γ4P retained the binding affinity and specificity for CD74 when compared with unconjugated hLL1, displayed RNase activity comparable with free Rap, showed potent *in vitro* cytotoxicity against CD74-positive (Daudi, Raji, and MC/CAR), but not CD74-negative (DMS 53), cell lines, and showed an excellent therapeutic index *in vivo* in two xenograft models of non–Hodgkin lymphoma (9). In this work, we provide a further example to illustrate that the NH_2-terminal fusion of Rap(Q) to a tumor-targeting mAb is a valid and versatile approach to generate novel immunotoxins by showing that (Q)-hRS7 (*a*) can be produced in a mammalian host and purified to homogeneity, (*b*) retains the binding specificity and affinity of hRS7, as well as the RNase activity of Rap, (*c*) suppresses the proliferation of various Trop-2–expressing cancer cell lines at nanomolar concentrations *in vitro*, and (*d*) inhibits the growth of a human lung tumor xenograft *in vivo*. The selection of Rap(Q) over Rap as the fusion partner prevents the addition of carbohydrates to the fused L chain, which should render (Q)-hRS7 a more homogeneous product than 2L-Rap-hRS7 because only one band would be observed for the fused L chain on reducing SDS-PAGE. We also expect (Q)-hRS7 similar *in vitro* properties to 2L-Rap-hRS7 based on the results obtained for 2L-Rap-hLL1-γ4P and 2L-Rap(Q)-hLL1-γ4P (30).

Materials and Methods

Cell lines and cell culture

Cervical cancer line (ME-180), breast cancer lines (T-47D, MDA-MB-468, and SK-BR-3), prostate cancer lines (DU-145, PC-3, and 22Rv1), lung adenocarcinoma line (Calu-3), pancreatic cancer lines (Capan-1, BxPC-3, and AsPc-1), and ovarian cancer line (SK-OV-3) were obtained from the American Type Culture Collection and cultured at 37°C in 5% CO_2 in RPMI 1640 supplemented with 10% heat-inactivated fetal bovine serum, 2 mmol/L L-glutamine, 200 U/mL penicillin, and 100 μg/mL streptomycin. The cell lines were passaged for <6 months, and no authentication was done.

Antibodies and reagents

Milatuzumab (hLL1, anti-CD74), hRS7, recombinant Rap (rRap), and a mouse anti-Rap IgG were prepared in-house. FITC-, phycoerythrin (PE)-, or horseradish peroxidase (HRP)–conjugated goat anti-human (GAH) or goat anti-mouse (GAM) IgG, Fc-specific, antibodies were purchased from Jackson ImmunoResearch Laboratories. GAH IgG conjugated to Alexa Fluor 488, human transferrin (hTf) conjugated to Alexa Fluor 568, and Hoechst 33258 were acquired from Molecular Probes (Invitrogen). All restriction enzymes were obtained from New England Biolabs.

Vector construction

The construction of the plasmid *pdHL2-Rap-L-hLL1-γ4P* for expressing 2L-Rap-hLL1-γ4P has been described in detail (9). The expression vector *pdHL2-Rap (Q)-L-hLL1-γ4P* was derived from *pdHL2-Rap-L-hLL1-γ4P* by replacing *Rap* with *Rap(Q)*, and the plasmid *pdHL2-Rap (Q)-L-hRS7-γ1* for expressing (Q)-hRS7 was constructed by subcloning *Rap(Q)* gene from *pdHL2-Rap(Q)-L-hLL1-γ4P* into *pdHL2-hRS7-γ1* vector. Briefly, an EcoRV restriction site was introduced at the NH_2-terminal/5′ side of the *hRS7* V_L gene using suitable primers by PCR. The XbaI-EcoRV fragment of *pdHL2-Rap(Q)-L-hLL1-γ4P* containing *Leader peptide-Rap-Linker* was ligated with the EcoRV-BamHI fragment generated by PCR containing *hRS7* V_L gene into an intermediate vector, *pBS-Rap(Q)-L-hRS7*. The Xba-BamHI fragment of *pdHL2-hRS7-γ1* was replaced with Xba-BamHI fragment of *pBS-Rap(Q)-L-hRS7*.

Transfection and selection

The *pdHL2-Rap(Q)-L-hRS7-γ1* vector (30 μg) was linearized with SalI and transfected by electroporation into Sp2/0 cells, which were grown in complete hybridoma serum–free medium supplemented with 10% low-IgG fetal bovine serum, 100 U/mL penicillin and 100 μg/mL streptomycin, 2 mmol/L L-glutamine, 1 μmol/L sodium pyruvate, 100 μmol/L essential amino acids, and 0.05 μmol/L methotrexate. Culture supernatants from wells of surviving cells were analyzed for the expression of the fusion protein by ELISA using HRP-conjugated GAH IgG, Fc-specific, antibody. Positive clones were expanded and frozen for future use.

Expression and purification

Cells were grown in roller bottles to terminal culture (10–20% viability). The supernatant was filtered and applied to a Protein A column, previously equilibrated with a pH 8.5 buffer containing 20 mmol/L Tris-HCl and 100 mmol/L NaCl. Following loading, the column was washed with a 100-mmol/L sodium citrate buffer (pH 7.0) and eluted with 100 mmol/L sodium citrate buffer (pH 3.5) to obtain the fusion protein. The peak containing the product was adjusted to pH 7.0 using 3 mol/L Tris-HCl (pH 8.5) and dialyzed against 40 mmol/L PBS. Following concentration, the product was filtered through 0.22-μm filters and stored at 2°C to 8°C.

Size-exclusion high-performance liquid chromatography and SDS-PAGE analyses

The purity and molecular integrity of (Q)-hRS7 was assessed by size-exclusion high-performance liquid chromatography using a Zorbax column purchased from Bio-Rad and by SDS-PAGE under reducing conditions using 4% to 20% Tris-glycine gels (PAGEr Gold Precast Gels).

In vitro transcription and translation assay

RNase activity was determined in a cell-free system by measuring the activity of *de novo* synthesized luciferase using the TNT Quick Coupled Transcription/Translation System (Promega) per manufacturer's instructions. Briefly, various test samples at concentrations ranging from 10 pmol/L to 100 nmol/L in 2 μL were added to 8 μL of the TNT Quick Master Mix containing methoinine and luciferase-control DNA, and incubated for 2 hours at 30°C in a 96-well, round-bottomed plate from which 2 μL were removed for analysis with 50 μL Bright-Glo substrate in a black 96-well, flat-bottomed plate. Plates were read on an Envision chemiluminescence reader. Relative luciferase units were plotted against the concentration of test samples.

Yeast tRNA degradation assay

RNase activity was also determined by measuring the amount of perchloric acid–soluble nucleotides formed using yeast tRNA (Invitrogen) as substrate (8). Each sample was prepared with RNase-free water (Ambion) in a 1.5-mL RNase-free Eppendorf tube to contain, in a final volume of 100 μL, 5 nmol/L (Q)-hRS7 or rRap, 10 mmol/L HEPES (pH 6.0), 200 μg/mL human serum albumin, and a predetermined concentration of tRNA ranging from 100 μg/mL (3.09 μmol/L) to 600 μg/mL (18.54 μmol/L). The enzymatic reaction was done at 37°C for 2 hours and terminated by adding 233 μL of 3.4% ice-cold perchloric acid to each sample on ice. After 10 minutes, samples were centrifuged in a microcentrifuge at 12,000 rpm for 10 minutes in the cold room. An aliquot was removed from the supernatant of each sample and diluted 10-fold with water, from which the absorbance at 260 nm was measured against water as blank. The initial rates were calculated for each substrate concentration by dividing the corresponding absorbance value with the reaction time (7,200 s) and plotted against the substrate concentrations to determine k_{cat}/K_m, which under the conditions of $K_m >> [S]$ according to the Michaelis-Menten equation should equal to the slope of the resulting least square line divided by the total enzyme concentration [5 nmol/L for rRap and 10 nmol/L for (Q)-hRS7].

Cell binding measurements

An ELISA-based method was used to evaluate binding of (Q)-hRS7 to select cell lines as follows. Cells were plated into a black 96-well, flat-bottomed plate (1×10^5 cells/well; 100 μL/well) and incubated overnight at 37°C in a 5% CO_2 humidified incubator. The next day,

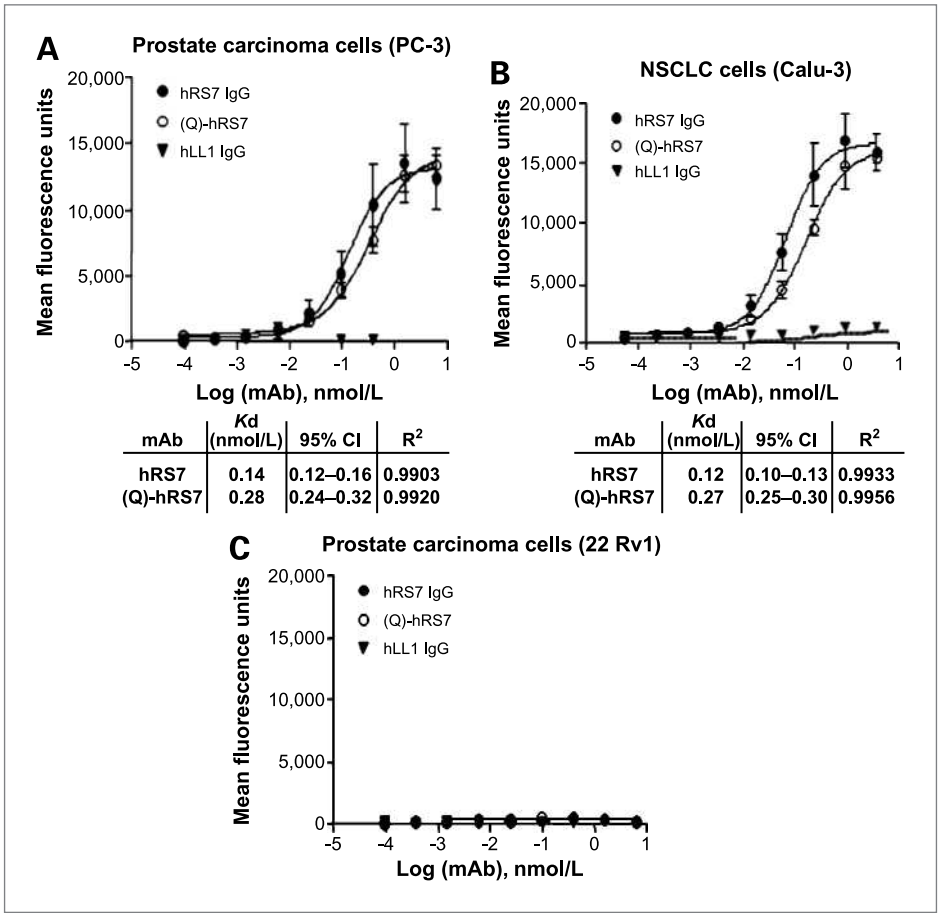

Figure 2. Cell binding curves obtained for PC-3 (A), Calu-3 (B), and 22Rv1 (C) from ELISA using the luminol substrates. The mean fluorescence units were plotted against concentrations, and the resulting data were analyzed by Prism software to obtain the values of K_D.

plates containing the cells were removed from the incubator and the media were flicked out of the wells followed by gentle patting dry on paper towels. Each well then received 50 μL of fresh growth media. Serial 1:4 dilutions (200–1.9 × 10^{-4} nmol/L) of (Q)-hRS7 were made in assay media (RPMI 1640; 10% fetal bovine serum complete media) and added (50 μL/well) in triplicates to corresponding wells (final concentrations, 100–0.95 × 10^{-4} nmol/L). After incubation for 1.5 hours at 4°C, the plates were centrifuged at 600 × *g* for 2 minutes, blotted dry on paper towels after removal of the media, and washed by adding 150 μL of ice-cold media into each well followed by centrifugation at 600 × *g* for 2 minutes. The media were removed, and the plates were blotted dry. HRP-conjugated GAH antibody was used at a 1:20,000 dilution and was then added to all the wells (100 μL/well). For background control, one set of wells received only cells plus the secondary antibody. The plate was incubated for 1 hour at 4°C. Afterwards, the plate was centrifuged and blotted dry. The cells were then washed twice with ice-cold media followed by a third wash with ice-cold PBS. The procedures of centrifugation, media removal, and plate blotting were repeated following each wash. After the last washing step, LumiGLO (KPL) was added to all wells (100 μL/well), and the plate was read for luminescence using an Envision plate reader. Data were analyzed using the GraphPad Prism software to determine the apparent affinity, which is the concentration corresponding to half-maximal saturation. In each experiment, hRS7 and hLL1 were included as positive and isotype controls, respectively.

Alternatively, binding of (Q)-hRS7 to human cancer cell lines was determined by flow cytometry on a Guava PCA (Guava Technologies, Inc.) using the manufacturer's reagents, protocols, and software. Similar studies were done in parallel for each cell line with hRS7 and hLL1. Briefly, ~5 × 10^5 cells of the various lines to be analyzed were obtained and resuspended in PBS/1% bovine serum albumin (BSA). Cells were centrifuged; resuspended in 100 μL of PBS/1% BSA containing 10 μg/mL (Q)-hRS7, hRS7, or hLL1; and incubated at 4°C for 45 minutes. After washing twice with PBS/1% BSA, with each wash followed by centrifugation, cells were resuspended in 50 μL of FITC-conjugated GAH, Fc-specific, antibody (1:25 dilution) and incubated for 30 minutes at 4°C. Cells were analyzed by flow cytometry after washing twice with PBS/1% BSA and resuspended in 0.5 mL of PBS/1% BSA. To separate dead from viable cells, 1 μg/mL of propidium iodide was added. For each analysis, 10,000 cells were acquired.

Cell proliferation assay

Tumor cells were seeded in 96-well plates (1×10^4 cells per well) and incubated with test articles at 0.01 to 100 nmol/L for 72 hours. The number of living cells was then determined using the soluble tetrazolium salt, MTS, following the manufacturer's protocol. The data from the dose-response curves were analyzed using the GraphPad Prism software to obtain EC_{50} values (the concentration at which 50% inhibition occurs).

Colony-formation assay

Tumor cells were trypsinized and plated in 60-mm dishes (1×10^3 cells). Cells were treated with each test article and allowed to form colonies. Fresh media containing the test article were added every 4 days, and after 2 weeks of incubation, colonies were fixed in 4% formaldehyde and stained with Giemsa. Colonies of >50 cells were enumerated under a microscope.

Internalization studies by fluorescence microscopy

ME-180 cells were placed (2,000 cells in 500 μL per well) in 8-well, Lab-Tek II chamber slides (Nalge Nunc International) and incubated with (Q)-hRS7 (10 μg/mL) or hRS7 (6 μg/mL) at 37°C for 16 hours. All subsequent steps were done at room temperature. After washing twice with PBS/2% BSA or twice with PBS/2% BSA followed by twice washing with 0.1 mol/L glycine (pH 2.5, 500 μL, 2 min), cells were fixed in 4% formalin for 15 minutes; washed twice with PBS; then probed with a mouse anti-Rap mAb followed by PE-conjugated GAM, Fc-specific, antibody, or directly with FITC-conjugated GAH, Fc-specific, antibody to reveal the location of (Q)-hRS7 or hRS7 using a fluorescence microscope.

A second study to address the subcellular location of (Q)-hRS7 was done as follows. Alexa Fluor 568–conjugated hTf was added with (Q)-hRS7 (10 μg/mL) or hRS7 (6 μg/mL) to MDA-MB-468 human breast cancer cells placed (3,000 cells in 500 μL per well) in eight-well chamber slides. After incubation at 37°C for 2 hours, cells were washed and fixed as described above, then treated with Alexa Fluor 488–conjugated GAH IgG for 15 minutes at room temperature. After washing twice with PBS, cells were treated with Hoechst 33258 for 15 minutes at room temperature, washed, and examined under a fluorescence microscope.

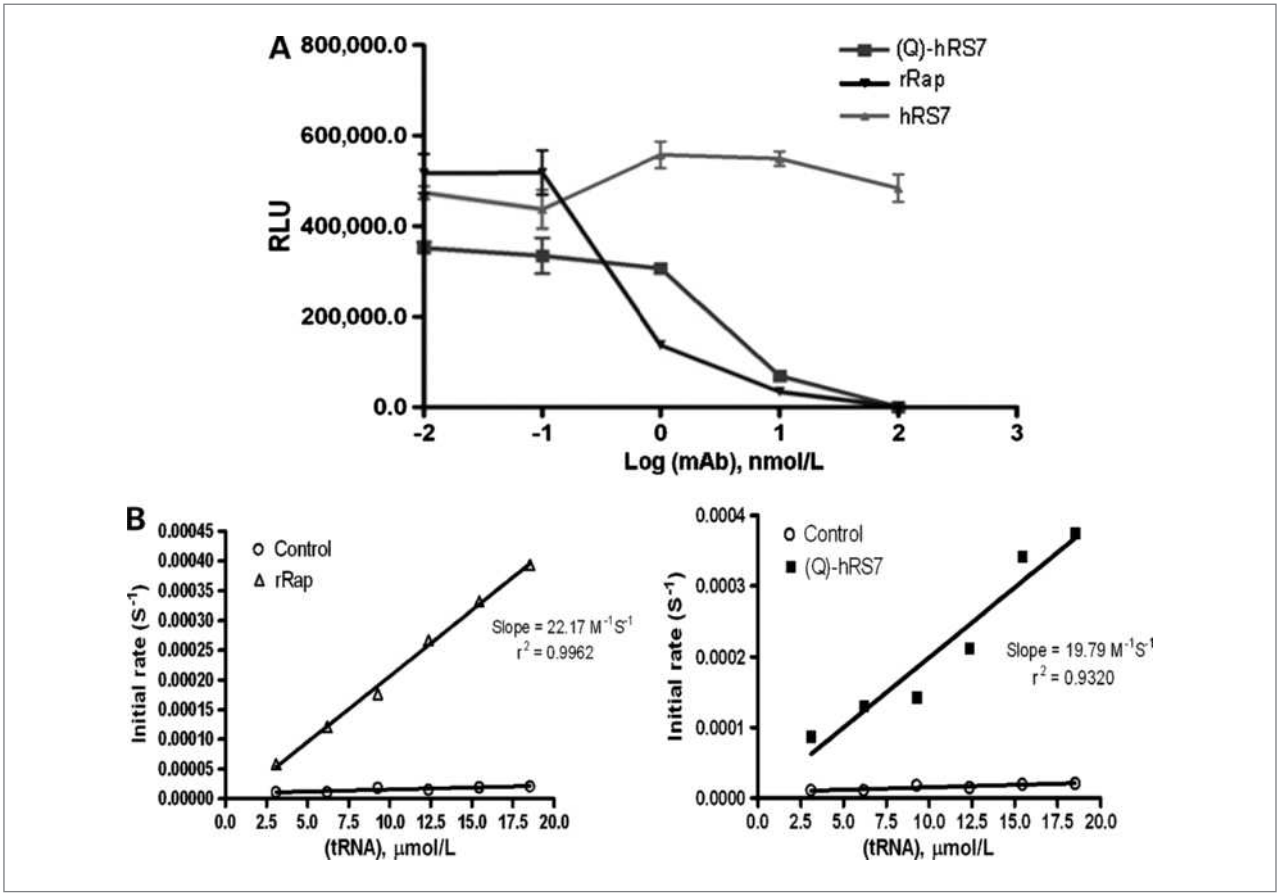

Figure 3. Representative data of the *in vitro* transcription and translation assay (A) showing (Q)-hRS7 and rRap have comparable RNase activity. B, plotting the initial rates of rRap (left) and (Q)-hRS7 (right) against the concentrations of yeast tRNA to determine k_{cat}/K_m.

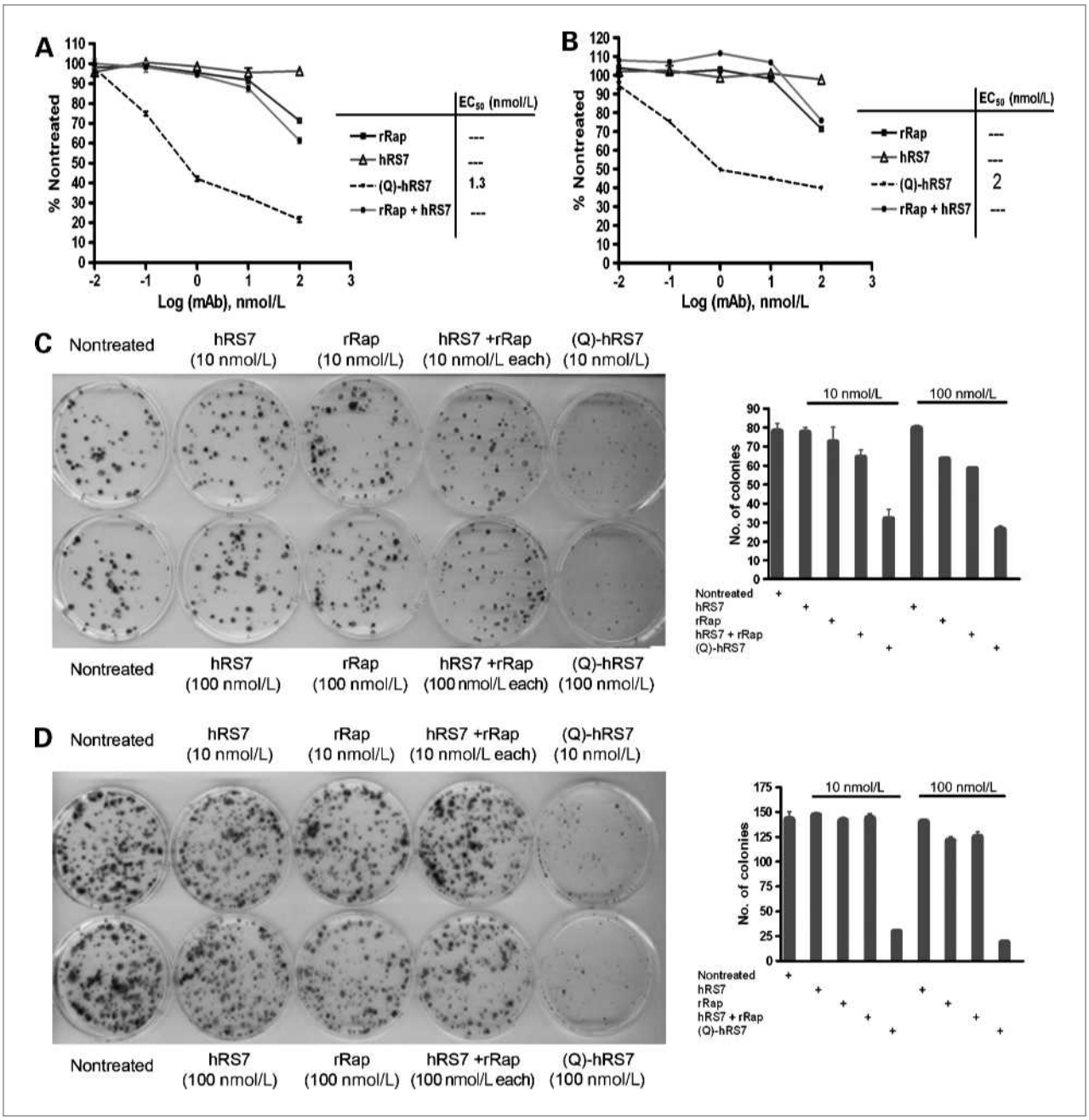

Figure 4. *In vitro* cytotoxicity of (Q)-hRS7 as evidenced by the MTS assay shown for ME-180 (A) and T-47D (B), and the colony formation assay shown for DU-145 (C) and PC-3 (D). The data in (A) and (B) were analyzed using the Prism software to obtain the values of EC_{50}.

In vivo toxicity

Naïve BALB/c mice (female, ages 7 wk, Taconic Farms) were injected i.v. with various doses of (Q)-hRS7 ranging from 25 to 400 μg per mouse and were monitored daily for visible signs of toxicity and body weight change. The maximum tolerated dose (MTD) was defined as the highest dose at which no deaths occurred, and the body weight loss was 20% or less of pretreatment animal weight (~20 g). Animals that experienced toxic effects were euthanized.

Therapeutic efficacy in tumor-bearing mice

Female NCr homozygous athymic *nu/nu* mice of ~20 g (ages 5 wk when received from Taconic Farms) were inoculated s.c. with 1×10^7 Calu-3 human non–small cell lung carcinoma cells and monitored for tumor growth by caliper measurements of length × width of the tumor. Tumor volume was calculated as $(L \times W^2)/2$. Once tumors reached ~0.15 cm^3 in size, the animals were divided into treatment groups of five per group. Therapy consisted of either a single i.v. injection of 50 μg of

(Q)-hRS7 or two injections of 25 μg administered 7 days apart. A control group received saline. Animals were monitored daily for signs of toxicity, and were humanely euthanized and deemed to have succumbed to disease progression if tumors reached >2.0 cm^3 in size or became ulcerated. Additionally, if mice lost >20% of initial body weight or otherwise became moribund, they were euthanized. Survival data were analyzed using Kaplan-Meier plots (log-rank analysis) with the GraphPad Prism software. Differences were considered statistically significant at $P < 0.05$.

Results

Purity and molecular integrity

(Q)-hRS7 was shown by size-exclusion high-performance liquid chromatography to consist of a single peak (Fig. 1B) with the observed retention time (7.8 min) indicating a larger molecular size than IgG. The purity of (Q)-hRS7 was also supported by the observation of only two bands on reducing SDS-PAGE, 1 of ~50 kDa attributed to the heavy chain of hRS7 and the other of ~37 kDa attributed to the Rap(Q)-fused L chain (Supplementary Fig. S1, lane 8).

Binding analysis

The reactivity of (Q)-hRS7 with Trop-2–expressing cell lines was initially assessed by ELISA and shown for PC-3 (Fig. 2A) and Calu-3 (Fig. 2B), both yielding an apparent dissociation constant (K_D) ~2-fold higher than that of hRS7 (0.28 nmol/L versus 0.14 nmol/L). No binding was observed for the Trop-2–negative 22Rv1 (Fig. 2C). Subsequent studies were done by flow cytometry in a total of 10 Trop-2–expressing cell lines, and the results (summarized in Supplementary Table S1), indicate that there was virtually no difference in the binding property of (Q)-hRS7 from that of hRS7.

RNase activity

The *in vitro* transcription and translation assay measures the inhibition of protein synthesis due to mRNA degradation by RNase. As shown in Fig. 3A, (Q)-hRS7 and rRap have comparable RNase activity in this cell-free assay, whereas no enzymatic activity was observed for hRS7. Using yeast tRNA as substrate, we estimated the k_{cat}/K_m (10^9 M^{-1} s^{-1}) of rRap and (Q)-hRS7 to be 4.10 (±0.42) and 1.98, respectively. Thus, the catalytic efficiency of (Q)-hRS7 based on the concentration of Rap is ~50% of rRap, which was similar to the reported 40% catalytic efficiency of LL2-onconase compared with the native Rap (8). A plot of the initial rates versus the concentrations of tRNA from a representative set of experiments is shown in Fig. 3B.

In vitro cytotoxicity

Based on the results of the MTS assay, (Q)-hRS7 is most potent against ME-180 (Fig. 4A), T-47D (Fig. 4B), MDA-MB-468, and Calu-3, with EC_{50} values of 1.5, 2.0,

Table 1. *In vitro* cytotoxicity of (Q)-hRS7

Cancer type	Cell line	Trop-2	MTS assay		Colony formation assay	
			EC_{50} (nmol/L)	% inhibition at 100 nmol/L*	% inhibition at 10 nmol/L†	% of inhibition at 100 nmol/L†
Prostatic	DU 145	+	>100	30	50	65
	PC-3	+	>100	29	80	90
	22 Rv1	–	>100	–5	0	0
Breast	MDA-MB-468	+	3.8	85	ND	ND
	MCF7	+	>100	41	85	94
	T-47D	+	2.0	60	90	95
	SK-BR-3	+	>100	30	85	ND
Pancreatic	BxPC-3	+	>100	22	>95	>95
	Capan-1	+	>100	4	65	80
	AsPC-1	–	>100	–3	0	0
Lung	Calu-3	+	8.5	65	ND	ND
Cervical	ME-180	+	1.5	80	ND	ND
Ovarian	SK-OV-3	+	>100	32	75	ND

Abbreviation: ND, not determined.

*The numbers shown are calculated using the formula: % inhibition at 100 nmol/L = 100% – [% of viable cells in samples treated with 100 nmol/L of (Q)-hRS7 relative to that of the nontreated].

†The numbers shown are calculated using the formula: % inhibition = 100% – [% of colonies formed in samples treated with 10/100 nmol/L of (Q)-hRS7 relative to that of the colonies formed by nontreated samples].

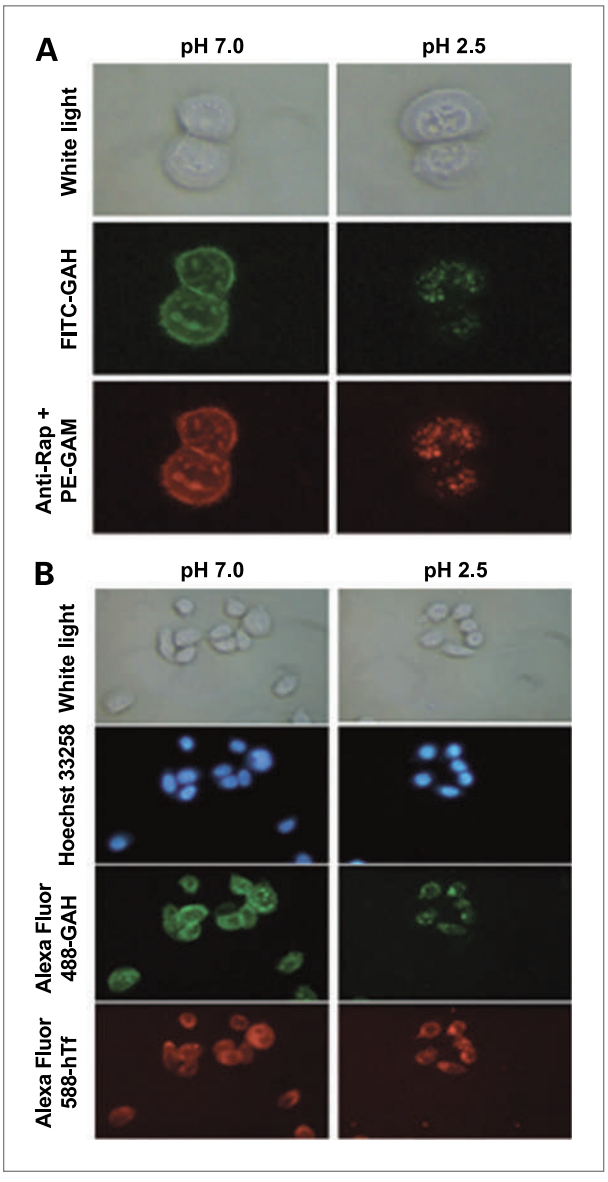

Figure 5. Internalization of (Q)-hRS7 in ME-180 (A) and in MDA-MB-468 (B). Left column, from cells washed with PBS-BSA (pH 7); right column, from cells washed with glycine (pH 2.5).

3.8, and 8.5 nmol/L, respectively. For those cell lines showing <50% growth inhibition at 100 nmol/L of (Q)-hRS7 with the MTS assay, we also did colony-formation assays to confirm that (Q)-hRS7 was cytotoxic at 10 or 100 nmol/L to DU-145, PC-3, MCF7, SK-BR-3, BxPC-3, Capan-1, and SK-OV-3. Representative results are shown for DU-145 (Fig. 4C) and PC-3 (Fig. 4D), with additional information provided in Table 1. It is noted that in both assays, the two Trop-2–negative cell lines, AsPC-1 and 22Rv1, were resistant to (Q)-hRS7. Moreover, hRS7, rRap, or the combination of hRS7 and rRap showed little, if any, toxicity at 100 nmol/L in all cell lines evaluated.

Internalization and subcellular location

The internalization of (Q)-hRS7 into ME-180 cells is clearly revealed in Fig. 5A for samples that were fixed after washing with PBS/0.2% BSA (middle and bottom, left column) or with a low-pH glycine buffer to strip membrane-bound proteins (middle and bottom, right column). The distribution pattern of intracellular (Q)-hRS7 in ME-180, as detected directly by FITC-conjugated GAH or indirectly by PE-conjugated GAM through mouse anti-Rap IgG, seems to be nearly identical, suggesting that (Q)-hRS7 remains intact following entry into these cells. The subcellular location of (Q)-hRS7 was further probed in MDA-MB-468 cells using fluorescence-labeled hTf as a marker for the recycling endosome and Hoechst 33258, which stains the nucleus. It is apparent from the results shown in Fig. 5B that (Q)-hRS7 and hTf occupy the same subcellular location in MDA-MB-468 when examined after incubation at 37°C for 2 hours. In both cell lines, hRS7 exhibited internalization characteristics similar to (Q)-hRS7, except that it was not visualized by PE-GAM/anti-Rap, as expected (data not shown).

MTD in mice

We have determined the MTD of (Q)-hRS7 in normal BALB/c mice given a single i.v. injection to be between 50 and 100 μg. Other 2L-Rap-X or 2L-Rap(Q)-X fusion proteins made to date have similar MTD range. In addition, we have determined the MTD of (Q)-hRS7 for multiple injections in naïve severe combined immunodeficient mice to be 80 μg by giving 20 μg every 5 days four times.

Therapeutic efficacy in tumor-bearing mice

As shown in Fig. 6A, either treatment (single dose, 50 μg or two doses of 25 μg given 5 d apart) with (Q)-hRS7 significantly inhibited the growth of Calu-3 xenografts compared with nontreated controls ($P < 0.019$), with the median survival time increased from 55 to 96 days ($P < 0.01$; Fig. 6B). In separate studies, we found hRS7 IgG was ineffective in Calu-3 as well as other Trop-2–expressing tumor xenografts when given at a dose of 500 μg twice weekly for 4 weeks (data not shown).

Discussion

Compared with immunotoxins made from toxins of plant or bacterial origin (31), for which clinical trials in cancer therapy have been completed or are ongoing for quite a few (32–34), the advancement of antibody-targeted RNases, called ImmunoRNases (35, 36), is relatively moderate, with the majority developed for treating hematologic malignancies and the targeting components conferred by some forms of scFv (37). To date, ImmunoRNases have not been evaluated in patients with any cancer.

Two considerable challenges noted in the clinical development of plant or microbial immunotoxins, namely

undesirable toxicity and immunogenicity, may also face (Q)-hRS7 and need to be addressed at the preclinical level and, eventually, clinically. Normal tissue toxicity observed with these immunotoxins includes vascular leak syndrome, hemolytic uremic syndrome, and hepatotoxicity (34). Because the structural motif (x)D(y) identified to be responsible for the binding of ricin A-chain or interleukin 2 to endothelial cells is absent in the native sequence of Rap(Q), and hRS7 is not cross-reactive with human endothelial cells, we consider the likelihood of (Q)-hRS7 causing vascular leak syndrome is remote. The large size of (Q)-hRS7 (~180 kDa), which poses a potential concern for less rapid penetration of tumors (38), should prevent its clearance through kidneys and mitigate the risk for hemolytic uremic syndrome. As for hepatotoxicity, we note that BL22, a recombinant anti-CD22 immunotoxin composed of the disulfide-stabilized Fv of RFB4 fused to PE38, and similar immunotoxins such as LMB-2 [anti-Tac(Fv)-PE38], also had a very low MTD in mice due to nonspecific liver toxicity, yet BL22 has been reported to be safe and efficacious in clinical trials of patients with hairy-cell leukemia (39). Thus, the dose-limiting hepatotoxicy commonly observed in mice may be rarely manifested in humans (34). Immunogenicity, on the other hand, is a more general problem because nearly all genetically engineered immunotoxins that have been evaluated in cancer patients induced a strong humoral immune response, which shortens the serum half-life and prevents further administration, thus compromising their clinical use. Several approaches to reduce the immune response have been tested in experimental animals, with some success reported for deoxyspergualin (40) and CTLA4Ig (41), and clinical testing of these and other immunosuppressive agents in combination with immunotoxins has been proposed (42). We expect to gain an initial insight into the potential immunogenicity of (Q)-hRS7 with future studies in Cynomolgus monkeys, which may also reveal whether there is an antigen sink for hRS7. However, we believe that (Q)-hRS7 should be less immunogenic because it comprises the fusion of a humanized antibody to a toxin that seems to induce little antibody response in patients (6).

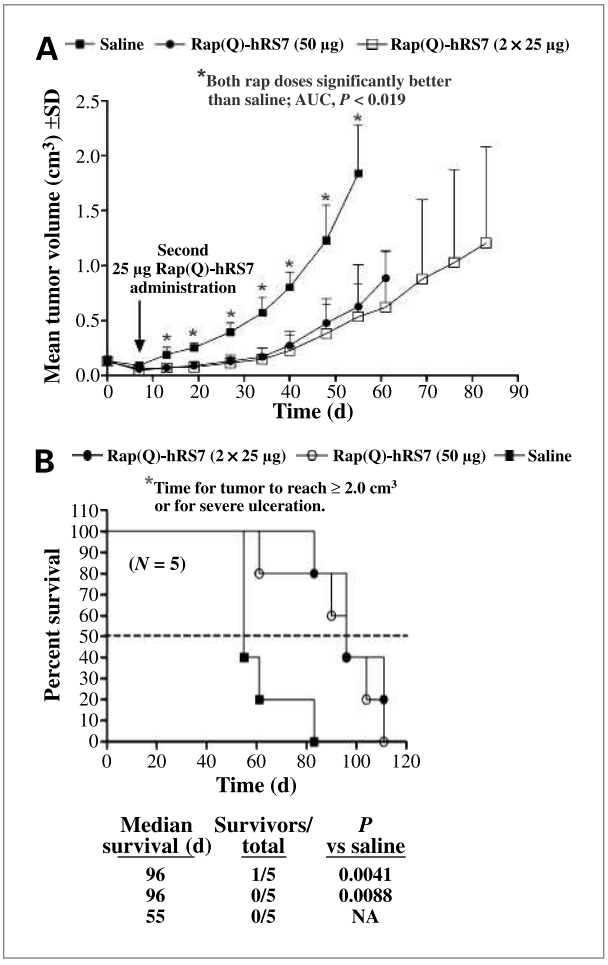

Figure 6. Therapeutic efficacy of (Q)-hRS7 shown in Calu-3 human xenograft model to inhibit tumor growth (A) and increase MST (B). Nude mice were inoculated s.c. with 1 × 10^7 Calu-3 cells. When tumors reached ~0.15 cm^3, mice were treated with either a single i.v. dose of 50 μg or two injections of 25 μg administered 7 d apart. Control animals received saline.

The cytotoxicity of 2L-Rap-X or 2L-Rap(Q)-X requires its entry into the target cell with subsequent translocation to the cytosol, in which Rap or Rap(Q) acts on tRNA and induces apoptosis and cell death (43). Although the intracellular pathways following internalization have been reported for Rap (44–46) and other RNases (46–48), as well as for ImmunoRNases comprising human pancreatic RNase fused to either a human anti-ErbB2 scFv (36, 49) or a human anti-CD30 scFv-Fc (50), a complete understanding is yet to emerge. Our internalization experiments indicate that (Q)-hRS7 is colocalized with hTf when examined at 2 hours after adding to MDA-MB-468, suggesting that (Q)-hRS7 may exit directly from endosomes into the cytosol, as proposed for Rap (45). The close resemblance of the fluorescence images observed in ME-180 for intracellular (Q)-hRS7 between anti-Rap and anti-human Fc further suggests the ability of (Q)-hRS7 to resist degradation by proteases during the endocytic process. Although the *in vitro* potency of (Q)-hRS7 was found to vary among Trop-2–expressing cell lines when measured by the 3-day MTS assay, which may be partially attributed to differential intracellular routing, the cytotoxicity of (Q)-hRS7 was unequivocally shown at 10 nmol/L for all cell lines using the 14-day colony-formation assay.

In addition to its potent cytotoxicity against diverse cancer cell lines *in vitro*, (Q)-hRS7 was shown to be effective in inhibiting the growth of Calu-3 human lung cancer xenografts in nude mice, thus validating the antitumor activity and stability of (Q)-hRS7 *in vivo*, as well as confirming the suitability of adding Trop-2 to the current list of antigens on solid cancers targeted by immunotoxins (31–33, 37).

In conclusion, we have shown that an amphibian RNase recombinantly fused with a humanized anti–Trop-2 antibody shows selective and potent cytotoxicity against a variety of epithelial cancers, both *in vitro* and *in vivo*. We believe this is a novel therapeutic candidate for clinical development.

Disclosure of Potential Conflicts of Interest

All authors have employment, stock, and/or stock options with Immunomedics, Inc.

Received 04/08/2010; revised 06/04/2010; accepted 06/23/2010; published OnlineFirst 07/27/2010.

References

1. Lee I. Ranpirnase (Onconase), a cytotoxic amphibian ribonuclease, manipulates tumor physical parameters as a selective killer and a potential enhancer for chemotherapy and radiation in cancer therapy. Exp Opin Biol Ther 2008;8:813–27.
2. Ardelt W, Shogen K, Darzynkiewicz Z. Onconase and Amphinase, the antitumor ribonucleases from Rana pipiens oocytes. Curr Pharm Biotechnol 2008;9:215–25.
3. Lee JT, Raines RT. Ribonucleases as novel chemotherapeutics. The ranpirnase example. Biodrugs 2008;22:53–8.
4. Costanzi J, Sidransky D, Navon A, Goldsweig H. Ribonucleases as a novel pro-apoptotic anticancer strategy: review of the preclinial and clinical data for ranpirnase. Cancer Invest 2005;23:643–50.
5. Mutti L, Gaudino G. The therapeutic potential of the novel ribonuclease ranpirnase (Onconase) in the treatment of malignant mesothelioma. Oncol Rev 2008;2:61–5.
6. Mikulski SM, Costanzi JJ, Vogelzang NJ, et al. Phase II trial of a single weekly intravenous dose of ranpirnase in patients with unrsectable malignant mesothelioma. J Clin Oncol 2002;20:274–81.
7. Mikulski SM, Grossman AM, Carter PW, Shogen K, Costanzi JJ. Phase I human clinical trial of onconase (P-30 protein) administered intravenously on a weekly schedule in cancer patients with solid tumors. Int J Oncol 1993;3:57–64.
8. Newton DL, Hansen HJ, Mikulski SM, Goldenberg DM, Rybak SM. Potent and specific antitumor effects of an anti-CD22-targeted cytotoxic ribonuclease: potential for the treatment of non-Hodgkin lymphoma. Blood 2001;97:528–35.
9. Chang CH, Sapra P, Vanama SS, Hansen HJ, Horak ID, Goldenberg DM. Effective therapy of human lymphoma xenografts with a novel recombinant rebonuclease/anti-CD74 humanized IgG4 antibody immunotoxin. Blood 2005;106:4308–14.
10. Stein R, Qu Z, Cardillo T, et al. Anti-proliferative activity of a humanized anti-CD74 monoclonal antibody, hLL1, on B-cell malignancies. Blood 2004;104:3705–11.
11. Aalberse RC, Schuurman J. IgG4 breaking the rules. Immunology 2002;105:9–19.
12. Liao Y-D, Wang S-S, Leu Y-J, et al. The structural integrity exerted by N-terminal pyroglutamate is crucial for the cytotoxicity of frog ribonuclease from *Rana pipiens*. Nucleic Acids Res 2003;31:5247–55.
13. Fornaro M, Dell'Arciprete R, Stella M, et al. Cloning of the gene encoding Trop-2, a cell-surface glycoprotein expressed by human carcinomas. Int J Cancer 1995;62:610–8.
14. Sewedy TE, Fornaro M, Alberti S. Cloning of the murine *TROP2* gene: conservation of a PIP_2-binding sequence in the cytoplasmic domain of TROP-2. Int J Cancer 1998;75:324–30.
15. Ripani E, Sacchetti A, Corda D, Alberti S. Human TROP-2 is a tumor-associated calcium signal transducer. Int J Cancer 1998;76:671–6.
16. Wang J, Day R, Dong Y, Weintraub SJ, Michel L. Identification of TROP-2 as an oncogene and an attractive therapeutic target in colon cancers. Mol Cancer Ther 2008;7:280–5.
17. Cubas R, Li M, Chen C, Yao Q. Trop2: a possible therapeutic target for late stage epithelial carcinomas. Biochim Biophys Acta 2009; 1796:309–14.
18. Huang H, Groth J, Sossey-Alaoui K, Hawthorn L, Beall S, Geradts J. Aberrant expression of novel and previously described cell membrane markers in human breast cancer cell lines and tumors. Clin Cancer Res 2005;11:4357–64.
19. Ohmachi T, Tanaka F, Mimori K, Inoue H, Yanaga K, Mori M. Clinical significance of *TROP2* expression in colorectal cancer. Clin Cancer Res 2006;12:3057–63.
20. Fang YJ, Lu ZH, Wang GQ, et al. Elevated expression of MMP7, TROP2, and survivin are associated with survival, disease recurrence, and liver matastasis of colon cancer. Int J Colorectal Dis 2009;24:875–84.
21. Fong D, Spizzo G, Gostner JM, et al. TROP2: a novel prognostic marker in squamous cell carcinoma of the oral cavity. Modern Pathol 2008;21:186–91.
22. Goldstein AS, Lawson DA, Cheng D, Sun W, Garraway IP, Witte ON. Trop2 identifies a subpopulation of murine and human prostate basal cells with stem cell characteristics. Proc Natl Acad Sci U S A 2008; 105:20882–7.
23. Stein R, Chen S, Sharkey RM, Goldenberg DM. Murine monoclonal antibodies raised against human non-small cell carcinoma of the lung: specificity and tumor targeting. Cancer Res 1990;50: 1330–6.
24. Stein R, Basu A, Chen S, Shih LB, Goldenberg DM. Specificity and properties of Mab RS7-3G11 and the antigen defined by this pancarcinoma monoclonal antibody. Int J Cancer 1993;55: 938–46.
25. Stein R, Basu A, Goldenberg DM, Looyd KO, Mattes MJ. Characterization of cluster 13: the epithelial/carcinoma antigen recognized by MAb RS7. Int J Cancer 1994;8:98–102.
26. Stein R, Blumenthal R, Sharkey RM, Goldenberg DM. Comparative biodistribution and radioimmunotherapy of monoclonal antibody RS7 and its $F(ab')_2$ in nude mice bearing human tumor xenografts. Cancer 1994;73:816–23.
27. Shih LB, Xuan H, Aninipot R, Stein R, Goldenberg DM. *In vitro* and *in vivo* reactivity of an internalizing antibody, RS7, with human breast cancer. Cancer Res 1995;55:5857–63s.
28. Stein R, Govindan SV, Chen S, et al. Reed. Radioimmunotherapy of a human lung cancer xenograft with monoclonal antibody RS7: evaluation of ^{177}Lu and comparison of its efficacy with that of ^{90}Y and residualizing ^{131}I. J Nucl Med 2001;42:967–74.
29. Qu Z, Griffiths GL, Wegener WA, et al. Development of humanized antibodies as cancer therapeutics. Methods 2005;36:84–95.
30. Vanama SS, Sapra P, Hansen HJ, Horak ID, Goldenberg DM, Chang C-H. Construction and characterization of two recombinant immunotoxins consisting of glycosylated and non-glycosylated ranpirnase fused to an internalizing anti-CD74 humanized IgG4 antibody [Abstract]. Cancer Biother Radiopharm 2004;19:514.
31. Kreitman RJ. Immunotoxins for targeted cancer therapy. AAPS J 2006;8:E532–51.
32. Pastan I, Hassan R, FitzGerald DJ, Kreitman RJ. Immunotoxin therapy of cancer. Nat Rev Cancer 2006;6:559–65.
33. Pastan I, Hassan R, FitzGerald DJ, Kreitman RJ. Immunotoxin treatments of cancer. Annu Rev Med 2007;58:221–37.
34. Kreitman RJ. Recombinant immunotoxins containing truncated bacterial toxins for the treatment of hematologic malignancies. BioDrugs 2009;23:1–13.
35. De Lorenzo C, Nigro A, Piccoli R, D'Alessio G. A new RNase-based immunoconjugate selectively cytotoxic for ErbB2-expressing cells. FEBS Lett 2002;516:208–12.
36. De Lorenzo C, Arciello A, Cozzolino R, et al. A fully human antitumor immunoRNase selective for ErbB2-positive carcinomas. Cancer Res 2004;64:4870–4.
37. Schirrmann T, Krauss J, Arndt MAE, Rybak SM, Dübel S. Targeted therapeutic RNases (ImmunoRNases). Exp Opin Biol Ther 2009;9: 79–95.
38. Yokota T, Milenic DE, Whitlow M, Schlom J. Rapid tumor penetration

of a single-chain Fv and comparison with other immunoglobulin forms. Cancer Res 1992;52:3402–8.
39. Kreitman RJ, Squires DR, Stetler-Stevenson M, et al. Efficacy of the anti-CD22 recombinant immunotoxin BL-22 in chemotherapy-resistant hairy-cell leukemia. N Engl J Med 2001;345:241–7.
40. Pai LH, FitzGerald DJ, Tepper M, Schacter B, Spitalny G, Pastan I. Inhibition of antibody response to Pseudomonas exotoxin and an immunotoxin containing Pseudomonas exotoxin by 15-deoxyspergualin in mice. Cancer Res 1990;50:7750–3.
41. Siegall CB, Haggerty HG, Warner GL, et al. Prevention of immunotoxin-induced immunogenicity by coadministration with CTLAIg enhances antitumor efficacy. J Immunol 1997;159: 5168–73.
42. Frankel AE. Reducing the immune response to immunotoxin. Clin Cancer Res 2004;10:13–5.
43. Iordanov MS, Ryabinina OP, Wong J, et al. Molecular determinants of apoptosis induced by the cytotoxic ribonuclease onconase: evidence for cytotoxic mechanisms different from inhibition of protein synthesis. Cancer Res 2000;60:1983–94.
44. Rodriguez M, Torrent G, Bosch M, et al. Intracellular pathway of onconase that enables its delivery to the cytosol. J Cell Sci 2007; 120:1405–11.
45. Haigis MC, Raines RT. Secretory ribonucleases are internalized by a dynamin-independent endocytic pathway. J Cell Sci 2003;116: 313–24.
46. Wu Y, Saxena SK, Ardelt W, et al. A study of the intracellular routing of cytotoxic ribonucleases. J Biol Chem 1995;270:17476–81.
47. Leich F, Stöhr N, Bietz A, Ulbrich-Hofmann R, Arnold U. Endocytic internalization as a crucial factor for the cytotoxicity of ribonucleases. J Biol Chem 2007;282:27640–6.
48. Bracale A, Spalletti-Cernia D, Mastronicola M, et al. Essential stations in the intracellular pathway of cytotoxic bovine seminal ribonuclease. Biochem J 2002;362:553–60.
49. De Lorenzo C, Di Malta C, Cali G, Troise F, Nitsch L, D'Slessio G. Intracelluar route and mechanism of action of ERB-hRNase, a human anti-ErbB2 anticancer immunoagent. FEBS Lett 2007;581: 296–300.
50. Menzel C, Schirmann T, Konthur Z, Jostock T, Dübel S. Human antibody RNase fusion protein targeting CD30+ lymphomas. Blood 2008;111:3830–7.